



Published in final edited form as:

Ann Biomed Eng. 2013 November ; 41(11): . doi:10.1007/s10439-013-0844-0.

Near Infrared Spectroscopic Evaluation Of Water In Hyaline Cartilage

MV Padalkar¹, RG Spencer², and N Pleshko^{1,*}

¹Department of Bioengineering, Temple University, Philadelphia PA, 19122

²National Institute on Aging, National Institutes of Health, Baltimore MD, 21224

Abstract

In diseased conditions of cartilage such as osteoarthritis, there is typically an increase in water content from the average normal of 60–85% to greater than 90%. As cartilage has very little capability for self-repair, methods of early detection of degeneration are required, and assessment of water could prove to be a useful diagnostic method. Current assessment methods are either destructive, time consuming or have limited sensitivity. Here, we investigated the hypotheses that non-destructive near infrared spectroscopy (NIRS) of articular cartilage can be used to differentiate between free and bound water, and to quantitatively assess water content. The absorbances centered at 5200 cm^{-1} and 6890 cm^{-1} were attributed to a combination of free and bound water, and to free water only, respectively. The integrated areas of both absorbance bands were found to correlate linearly with the absolute water content ($R=0.87$ and $R=0.86$) and with percent water content ($R=0.97$ and $R=0.96$) of the tissue. Partial least square models were also successfully developed and were used to predict water content, and percent free water. These data demonstrate that NIRS can be utilized to quantitatively determine water content in articular cartilage, and may aid in early detection of degenerative tissue changes in a laboratory setting, and with additional validations, possibly in a clinical setting.

Keywords

Water; Cartilage; Near infrared (NIR) spectroscopy; Partial least squares (PLS) Regression

Introduction

Articular cartilage is a hyaline cartilage that lines the subchondral bone in a diarthrodial joint. The composition of articular cartilage varies throughout the depth, with water content being greatest at the surface and lower in the deeper zone⁴⁹. The primary functions of water in cartilage are shock absorption during loading, transport of nutrients and lubrication. Therefore the study of transport of water molecules within the cartilage has gained importance and has been studied for over 40 years^{41; 59}. The type of water in cartilage has generally been categorized as existing in three pools, as free water, water that forms hydrogen bonds with the collagen surface and trapped between collagen fibers (tightly bound), and water that forms hydrogen bonds with proteoglycan anionic sites (loosely bound)^{30; 58}.

Osteoarthritis (OA) is a progressively disabling musculoskeletal disease characterized by degeneration of articular cartilage. Approximately 21 million adults in the United States

over the age of 45 years have been estimated to have the disease³², with prevalence directly correlated to age. In diseased conditions such as OA there is an increase in water content from the average normal of 60–85% to greater than 90%²⁸. It is thought that this increase is attributable to a denatured collagen network leads to decreased proteoglycan content^{42; 48; 62} which results in increased water in the tissue matrix. As cartilage has very little capability for self-repair due to low turnover rate of the cells and its avascular nature, methods of early detection of degeneration are required¹⁷. Several recent studies have investigated methods to improve detection of OA, based on changes in water, matrix or mechanical properties. Examples include a study by Duda et al. where they described a novel medical device to detect early osteoarthritis based on assessment of the mechanical stiffness of cartilage²³, and magnetic resonance imaging (MRI) studies that evaluated degenerative cartilage based on changes in matrix and water content, which are more common. Although MRI suffers from relatively low spatial resolution, quantitative MRI (qMRI) techniques¹⁸, microscopic MRI (μ MRI)⁶⁴, MRI combined with Optical Coherence Tomography⁴⁶ and three dimensional MRI⁵³ are emerging as promising high resolution tools to detect osteoarthritis based on water and matrix changes. The MRI parameter transverse relaxation time T2 is associated with the water^{31; 38; 40; 47; 53}, but is not sensitive to small changes in water content. In addition, the fact that articular cartilage is very thin and has curved surfaces contributes to the insensitivity of some MRI analyses due to partial-volume averaging effects. This makes the detection of thin fissures, cartilage flaps, and shallow defects difficult⁵⁰. MRI studies have also had limited success in quantitation of biochemical changes in earlier stages of osteoarthritis²². Thus, even though the evaluation of water content changes in cartilage could be a useful strategy in early detection of OA, a sensitive non-or minimally invasive modality remains to be optimized.

The current 'gold standard' methods for water detection in tissues are gravimetric analysis⁵ and Karl Fischer titration¹⁵. Gravimetric analysis, although a relatively simple method based on obtaining wet and dry weights of a sample, is time consuming compared to Karl Fischer titration. The main disadvantage of Karl Fischer titration is that the material analyzed must dissolve in the titration medium to get an accurate water content assessment. However, since some biological tissues may bind with the reagents used in Karl Fischer titration, this could lead to inaccuracies in results. In addition, Karl Fischer titration measures bound as well as surface water, and therefore will result in a greater water content compared to gravimetric method. Further, both of these methods of water measurements are destructive, and therefore are not suitable in a clinical setting.

Near infrared spectroscopy (NIR) spectroscopy is an attractive non-destructive alternative for characterization and quantification of water in cartilage. The NIR spectrum consists of overtones and combination bands of the fundamental molecular vibrations found in the mid-infrared region. There are two dominant water peaks in the NIR region: centered at 5200 cm^{-1} and 6890 cm^{-1} , respectively^{34; 37}. Earlier and recent studies have utilized near infrared (NIR) spectroscopy in either a non or minimally invasive mode for analysis of water in food^{10; 45}, pharmaceuticals^{9; 66} and skin^{3; 4; 44}. Both the 5200 cm^{-1} and the 6890 cm^{-1} absorbances have been used for quantitation. In cartilage research, water quantitation based on the NIR absorbance bands has not yet been carried out. The first NIR probe study of cartilage or articular joints reported a preliminary evaluation of joint synovium¹⁶.

In the more recent literature, there have been several studies where NIR fiber optic probes have been used to assess cartilage quality. There have also been reports of assessment of severity of cartilage defects using a NIR probe. Spahn et al. conducted a series of NIR spectroscopy studies to evaluate the utility of this technique to assess cartilage defects^{55–57}. In one study, the ratio of a NIR water absorbance band at 7017.54 cm^{-1} to the 8510.64 cm^{-1} absorbance (a matrix absorbance) was considered as an indicator of water content⁵⁶.

Although they used a Karl-Fischer titration to determine water content of the cartilage, a direct correlation of NIR water absorbance bands and actual water content was not presented. The second study showed that NIR spectral data obtained from human cartilage had better intraobserver agreement for prediction of early cartilage disease than MRI or arthroscopy²⁷. Finally, Marticke et al. correlated NIR data with cartilage mechanical properties, showing a positive correlation between NIR spectra and Young's modulus for osteoarthritic cartilage⁴³. Together, these studies demonstrate the potential for NIR spectroscopy to aid in evaluation of cartilage matrix changes in a clinical environment.

Another series of studies by Brown demonstrated the correlation of NIR spectroscopic data to severity of cartilage degeneration in enzymatically degraded¹¹ and osteoarthritic tissues¹². In those studies, quantitative assessments of changes in tissue water content were also not performed. In a recent study from our group, water content in engineered cartilage, based on the 5200 cm⁻¹ absorbance band, was correlated to matrix composition⁸. However, to date, NIR spectroscopic assessment of water in cartilage has not been shown to correlate to the gold standard, gravimetric water determination, and therefore quantitative data on changes in water content have not been obtained. The current study aims to demonstrate the ability of NIR spectroscopic assessment to quantitatively predict water content in cartilage.

In addition to changes in total water content, changes in the relative amount of free and bound water in cartilage may also reflect tissue quality. As the increase in water content during disease progression is associated with the loss of proteoglycan and rupture of the collagen network, it is likely that the balance of free and bound water changes. In the current study, we hypothesized that NIR spectroscopy can be used to quantitatively assess water content and its' free or bound state in hyaline cartilage, providing further support for the use of this modality for assessment of early OA. To test this hypothesis, we investigated a model system of bovine nasal cartilage (BNC) tissue, which is a hyaline cartilage that is more homogeneous and isotropic compared to articular cartilage. Unlike articular cartilage, BNC has no zonal variation. Many studies on the progression of OA have utilized BNC for this reason^{35; 36; 65}, to avoid the zonal composition variation observed in articular cartilage which could be a confounding factor in data evaluation. The two aims of the study were to validate the assignments of "free" and "bound" water to the 6890 cm⁻¹ and 5200 cm⁻¹ absorbances, respectively, and to evaluate whether the NIR spectral bands that arise from water do indeed correlate to the water content in these materials. Two different approaches were used for data analysis: simple integrations of the areas of the water absorbances, and partial least squares (PLS) analysis.

Materials & Methods

Bovine nasal cartilage (BNC) tissues

Bovine nasal cartilage was collected from freshly slaughtered 2–3 month old animals, n= 2 (JBS, Souderton PA). Tissues were stored in phosphate buffered saline (10X, pH 7.4, Invitrogen, Carlsbad, CA) and Protease Inhibitor (Sigma Aldrich, St. Louis, MO) at -18°C until use, and allowed to come to room temperature before analysis. Plugs of 6 mm diameter were obtained with a biopsy punch, and sliced to either 0.5mm or 1 mm thickness, and weighed immediately to obtain wet weight. Following spectral data collection (described below), tissues were lyophilized for 20 hours at -50°C in vacuum (Labconco, Kansas City, MO) to obtain dry weight. NIR spectral data were also collected after lyophilization. For each sample (n = 5 for 0.5 mm and 1 mm) spectra were collected from 16 different regions across the tissue (details below).

NIR Spectroscopy

A Perkin Elmer Spotlight 400 imaging spectrometer (Perkin Elmer, Shelton CT), which couples an infrared spectrometer to a light microscope equipped with an array detector, was used to obtain NIR data in transmission mode in the frequency range from 4000–7800 cm^{-1} . Spectra from 1 mm slices of BNC placed on glass slides were obtained at 50 μ pixel resolution, and were used to investigate bound and free water. Spectral data were collected at 32 cm^{-1} spectral resolution with 32 co-added scans per pixel, with a total imaging time of less than 1 minute per sample. Penetration of the NIR radiation was through the entire 1 mm segment of tissue, and therefore, full-thickness sampling of all tissue components occurred. Transmittance spectra were ratioed to a background obtained through the glass slide and converted to absorbance for data analysis. For each tissue sampled, 16 spectra per image were acquired. BNC slices were imaged continually in intervals of 5 to 15 minutes over a three hour period to observe the spectral changes due to water evaporation, and to permit assignment of bound and free water absorbances. The 0.5 mm thick samples were imaged every 15 minutes for 2 hours keeping all parameters the same as for the 1 mm thick samples, and resulted in a total of 800 spectra. The NIR spectra obtained from these samples were used to assess correlations between integrated band areas and water content, and to build a partial least squares model to predict water content. Temperature and humidity were recorded for each experiment and ranged between 70F to 75F and 22–25% humidity for each experiment.

Data analysis: BNC water content

Tissues on the glass slides were weighed at each time point of data collection. The weight of the glass slide alone was subtracted, and for each time point during the course of evaporation of water from the tissues, the gravimetrically-determined absolute water content was calculated as:

$$\text{Absolute water content (mg)} = \text{Wet weight}_T - \text{Dry weight}_L, \quad (1)$$

Where, Wet weight_T = the tissue weight at a specific time point T

Dry weight_L = the weight of the tissue after lyophilization

$$\text{Percent water content} = \frac{\text{Wet weight}_T - \text{Dry weight}_L}{\text{Wet weight}} * 100 \quad (2)$$

Correlations

Integrated areas under the NIR water absorbances centered at 5200 cm^{-1} and 6890 cm^{-1} were calculated using ISYs 5.0 software (Malvern Instruments, UK). Correlations of the integrated areas of these absorbances with absolute and percent water content were assessed using a Pearson correlation with statistical significance determined at the $p < 0.05$ level.

Partial Least Squares Models

Partial least square (PLS) analysis is a statistical method used to find fundamental relationships between predictor and response variable. In the current study, PLS1 models (models built on a single y dependent variable) were evaluated for prediction of water from BNC tissues using The Unscrambler software (CAMO Software, Oslo, Norway). Second derivatives (Gap-Segment (Gap size 5 and Segment size 13)) and multiplicative scatter corrections (MSC) were used as pretreatments for all data sets. Multiplicative scattering correction (MSC) negates amplification and offset artifacts caused by light scattering, and

second derivatives are useful for removing baseline shifting and to discern overlapping peaks²⁴. The predictor matrix consists of rows of NIR spectra from the BNC samples, and the columns contain the absorbance values at each wavenumber, while the response matrix was created with either gravimetrically- determined % water content or absolute water content. From the 800 NIR BNC spectra collected over time as water evaporated, only spectral data that were not off-scale were included in the PLS model (some data from the initial timepoints were off-scale, with absorbances greater than 2 absorbance units). Lyophilized spectral data were also not included. This resulted in a total of ~672 spectra used in the PLS analysis. Unscrambler was used to randomly select 420 spectra to build the model and 252 spectra for prediction. This was repeated 3 times, where 420 spectra were randomly chosen each time, and the remaining 252 spectra used for independent prediction. The residual sum of squares error calculated from cross-validation (random 10 samples per segment) was used to determine the optimal number of factors. The presence of outlier spectra for each model was investigated using the Hotelling T² ellipse algorithm and influence plots of residual variance vs sample leverage²⁴, but no spectra were identified as outliers. The quality of the fit for each model was assessed by the coefficient of determination of validation (R²) and the root mean square error (RMSE). The root mean square error of prediction (RMSEP) was used to assess the quality of the prediction of the independent sample sets.

A separate PLS model for percent water was developed in the range of 50–80% water content to evaluate the performance of our model in the physiological range with 224 spectra and 112 spectra were used to test the performance of the model. Another PLS model was built to predict percent free water from the 0.5 mm thick BNC samples. The response matrix in this case was the percent free water calculated from the ratios of the integrated areas under the 5200 cm⁻¹ absorbance as described below:

$$\text{Percent free water} = \frac{\text{Integrated Area } T - \text{Integrated Area } L}{\text{Integrated Area } T} * 100 \quad (3)$$

Integrated Area_T = Integrated area under 5200 cm⁻¹ absorbance at specific time point (reflects total bound plus free water)

Integrated Area_L = Integrated area under 5200 cm⁻¹ absorbance of lyophilized sample (reflects total bound water)

Results

Assessment of free and bound water

The NIR absorbances at 5200 cm⁻¹ and 6890 cm⁻¹ decreased as the BNC samples dried over a three hour period (Figure 1A). Direct comparison of a spectrum obtained after one hour of evaporation and after lyophilization for 20 hours reveals that there is a negligible absorbance at 6890 cm⁻¹ in the lyophilized sample, which indicates that there is no longer any water present that contributes to that absorbance (Figure 1B). Thus, this absorbance band does indeed result from free water. The area of the 5200 cm⁻¹ band was also reduced during the evaporation process, but ~2 to 6% of the original absorbance still remained after lyophilization. These data indicate that there is indeed a bound water component, in addition to a free water component. The integrated areas in both NIR water absorbances decreased in a linear fashion through ~60 minutes of tissue drying (Figure 1C,D), and then began to level off. For both absorbances, a very slight increase in integrated area is observed at ~140 minutes, likely due to the fact that background spectrum was re-acquired at this timepoint.

Further spectral changes attributable to free and bound water were revealed by second derivative NIR spectra from BNC samples imaged at 5 minutes intervals during water evaporation (Figure 2). No change in peak position of the 6890 cm^{-1} was observed over time. However, the NIR absorbance band centered at 5200 cm^{-1} underwent a shift to lower frequencies as the water evaporated (Figure 2A). As the frequency of vibration depends on the mobility of water, a shift to lower frequency indicates less mobile, or more strongly bound water, and is further confirmation of the assignment of this absorbance band.

Correlations

The gravimetrically calculated absolute water content of the 0.5 mm thick BNC samples was in the range of 12 to 36 mg per sample, and the percent water content was in the range of 60–75%. The percent bound water was in the range of 1.65–6.59%. The integrated areas of the NIR absorbance bands at both 5200 cm^{-1} and 6890 cm^{-1} significantly correlated with percent water content ($R = 0.97$, $p < 0.01$ and $R = 0.96$, $p < 0.01$) (Figure 3A–3B) and with the absolute water content ($R = 0.87$, $p < 0.01$ and $R = 0.86$, $p < 0.01$) (Figure 3C–3D)

PLS prediction of water content

The PLS models were able to predict absolute water content with an average RMSEP of 2.89 mg, and percent water content with an average RMSEP of 5.81% (Table 1, Figure 4A). The PLS models to assess percent water content in the physiologic range of 50%–80% were able to predict the percent water content with an average RMSEP of 2.68%. In addition, percent free water was predicted with an average RMSEP of 2.52% (Table I, Figure 4B).

Discussion

The current study confirmed that NIR spectroscopy can be used to quantitatively assess water content in hyaline cartilage. Along with this primary objective, another objective was to confirm the assignment of free and bound water absorbances to the NIR absorbance bands centered at 6890 cm^{-1} and 5200 cm^{-1} . Liquid water occurs in different bound states in most materials and tissues, including cartilage, but for simplicity can be generally characterized as free or bound water. Free water is comprised of water in the liquid state present in large cavities or pores within solid material, whereas bound water is the water covalently bound or hydrogen bound to proteins or other molecules. Prior studies have attributed the 6890 cm^{-1} absorbance to free water³⁷, and the 5200 cm^{-1} absorbance to free and bound water^{6, 37, 52}. We found that these two prominent water peaks in the cartilage NIR spectrum actually reflect free water, and a combination of bound plus free water, respectively.

Interestingly, a study by Luck³⁷ also attributed the 5200 cm^{-1} band to a combination of free and bound water. They found the absorbance to arise from the sum of four different states of the water OH groups as follows: 1) $\sim 5446\text{ cm}^{-1}$, free molecules with hydrogens unbonded, 2) $\sim 5265\text{ cm}^{-1}$, molecules with one hydrogen bonded and the other unbonded; 3) $\sim 5165\text{ cm}^{-1}$, H-bonded OH-groups with energetically unfavored bond angles; 4) $\sim 5040\text{ cm}^{-1}$, H-bonded OH-groups with linear bonding³⁷. Our results are also consistent with the literature assignment of free water to the 6890 cm^{-1} absorbance in that same study. In addition, several other studies confirmed these assignments in other tissues and proteins. In one study on intact proteins, Vandermeulen et al.⁶⁰ assigned an absorbance band near $\sim 5260\text{ cm}^{-1}$ as free water, whereas the band near $\sim 5100\text{ cm}^{-1}$ was assigned to bound water. Ressler et al.⁵² concluded that the band near $\sim 5100\text{ cm}^{-1}$ exists even in tissue with the lowest water content (lyophilized); they therefore attributed this band to firmly bound water. Bagratasvili et al.⁶ used NIR spectroscopy to study the thermal diffusion process of water in nasal cartilage and concluded that the free and bound water spectra differed from each other and from the

spectrum of pure water based on the frequency. The $\sim 5200\text{ cm}^{-1}$ band representing free and bound water in cartilage was shifted by 12 cm^{-1} as compared to the $\sim 5200\text{ cm}^{-1}$. Zhou et al.⁶⁶ used PLS1 models to determine surface water and bound water in drying drug substances and confirmed that free water (surface water) absorbed at $\sim 5252\text{ cm}^{-1}$, and that bound water absorbed at $\sim 5165\text{ cm}^{-1}$ which is also in agreement with our results. Thus, we see here that the NIR absorbances from water in articular cartilage are similar to those in other materials and biological tissues.

We found that in BNC the bound water, which was not removed by lyophilization, averaged $3.72 \pm 1.97\%$ of the total water content. This pool of water is likely tightly bound to collagen, which is in agreement with the earlier study by Bagratavili et al.⁶, where they concluded that the proportion of bound water in rabbit nasal cartilage was $\sim 4\%$. Interestingly, Jaffe et al.³⁰ showed that less than 6% water was tightly bound to cartilage even after vacuum desiccation, and even lesser amount of water was bound to cartilage after heating at 98°C for four hours. The authors concluded that the tightly bound water may be trapped within the matrix, but likely bound to collagen rather than proteoglycans. This observation is also consistent with a study by Mankin et al.³⁹ based on water binding in normal and osteoarthritic cartilage in humans. They conclude that water in cartilage had a greater affinity for collagen than proteoglycans, and therefore the tightly bound water may be bound to collagen. A recent magnetic resonance spectroscopy study by Reiter et al.⁵¹ quantified the amount of water bound to proteoglycan and collagen macromolecules based on multiexponential water relaxation, and concluded that $\sim 6\%$ of the water was bound to collagen, whereas $\sim 14\%$ of the water was tightly bound to proteoglycan. Thus, the NIR data in the current study are in the same range as earlier studies. However, to fully understand exactly which macromolecules the bound water is associated with, further experiments, such as enzymatic degradation focused on specific components, can be performed.

The second derivative spectra acquired while the tissues were drying over time showed a low frequency shift in the position of the NIR absorbance band centered at $\sim 5200\text{ cm}^{-1}$, whereas no shift was observed in the 6890 cm^{-1} water band. In a previous study on water desorption from skin, Walling and Danbey reported a similar observation⁶¹. They found that the second derivative of the water absorbance from skin showed peak shifts from $\sim 5224\text{ cm}^{-1}$ to 5170 cm^{-1} as the water content from the skin decreased, and no shift was observed in any other band associated with NH, CO, or CH. These results support the concept that frequency of vibration of the water molecules is greater in the free water components as compared to the covalently or hydrogen-bound component, and could be useful for further studies to elucidate different water compartments in cartilage attributable to binding to different matrix molecules.

The results of the gravimetrically determined percent water content in the BNC samples were as expected, in the range of the physiological water content of the cartilage, 60 to 75%²¹. Both PLS models, using the full range of water values, and using only the physiological range of water values, were able to predict percent water with an error of ~ 5 to 8 percent of the total range of values. The positive correlation between the integrated areas under the NIR absorbances at 5200 cm^{-1} and 6890 cm^{-1} confirm our hypothesis that an increase in water content results in an increase in area under these NIR absorbances. Further, the strong correlation of the integrated areas of both bands with absolute water content of BNC samples indicate that either of these band areas can be used to predict water content from hyaline cartilage.

The use of non-invasive or minimally-invasive NIR evaluation of tissue quality is highly desirable from a clinical point of view for early detection of osteoarthritis. Although minimally invasive assessments of cartilage by mid-infrared spectroscopy have been used in

prior studies to evaluate matrix and correlate to tissue grade^{26; 33; 63}, most NIR studies of degraded cartilage have focused on qualitative evaluation of water absorbances. NIR fiber optic spectroscopy was used recently to distinguish between normal and enzymatically degraded cartilage and to detect early cartilage degeneration^{11; 12; 55}. Brown et al.¹¹ used PLS analysis of fiber optic diffuse reflectance NIR spectra and observed higher overall absorbance in enzymatically degraded cartilage, which they attributed to increased water content secondary to degradation. This was based on assessment of the entire spectrum and did not address quantification of water content or matrix components.

A further study by Brown et al.¹² concluded that diffuse reflectance NIRS can differentiate between normal, visibly normal (no fibrillation area next to defect), and degraded cartilage. This was based on a discriminating function developed from the NIR absorbance bands of water, where they observed that in normal tissue the 5150 cm^{-1} absorbance band (free plus bound water) is lower than the 7000 cm^{-1} absorbance band (free water), where as in degraded tissue it is higher¹². In the most recent study by that group¹³, they concluded that NIR spectroscopy was a better predictor of visibly normal osteoarthritic tissue in bovine patellae than mechanical indentation and ultrasound imaging. Here, they used the ratio of the water absorbance band at $\sim 5150 \text{ cm}^{-1}$ and the matrix absorbances at 4600–4900 cm^{-1} as an indicator for swelling due to early cartilage degeneration¹³. Together, these studies demonstrate the changes in water absorbances from cartilage in varying states of degradation, and the sensitivity of NIR spectra to those degradative changes.

Notwithstanding the results obtained here, there were some limitations to the current study, including lack of a precisely controlled humidity and temperature environment. In a previous study where water content from the skin was determined by NIR reflectance spectroscopy, it was found that the entire spectrum was shifted to higher absorbance values at high humidity, indicating an increase in tissue water content⁴⁴. Temperature changes can also influence NIR spectra, and studies have shown increases in intensity of the absorbance bands, shifts to higher frequencies, and band narrowing with increases in temperature^{19; 34; 37}. In the current study, data were acquired under similar temperature and humidity conditions to minimize the effect of these confounding variables. Ideally, a humidity controlled environment for water content assessment would be utilized. However, for clinical applications, it is necessary to confirm that NIR data are stable in the temperature and humidity conditions present during arthroscopic assessments. It may be possible to overcome this by use of a repeatability file¹⁴ with the existing model. A repeatability file is simply a group of spectra of cartilage acquired under varying humidity/water and temperature conditions taken over period of time. The purpose of this repeatability file is to make the calibration model more robust by minimizing the discrepancies caused by these variables. During standard arthroscopy procedures, the knee joint is filled with pressurized saline which rinses off the synovial fluid to give the surgeon a clear view of the cartilage, and keeps the joint open. In this case the probe will be surrounded by saline, which could result in interference from water external to the tissue. Future in-vivo experiments, such as those performed with cadaver knees using an arthroscopic setup, will be required to account for the contribution of external free water on the prediction of free water within the cartilage tissue.

Bovine nasal cartilage was used in these studies to avoid the zonal variation of articular cartilage, but this also results in a potential limitation of this model. Oriented collagen fibrils in articular cartilage may trap water differently compared to bovine nasal cartilage, and therefore the bound water could differ between the two cartilage types. Another limitation of the study was that data were collected from cartilage of the same known thickness in order to obtain absolute measures of water content as opposed to only proportional measures. In vivo, the relationship between the NIR water absorbances and the degenerative state of

cartilage will not be as straightforward. Cartilage thickness can decrease to a variable extent with degeneration, which would decrease the overall absorbance of any NIR absorbance band, or result in changes in band ratios, as shown by Brown et al. However more recently the spectral variations were used to determine thickness, and this could be useful methodology during clinical evaluation². Although the system used here was standardized for thickness, it nevertheless demonstrates the feasibility of obtaining quantitative data on water content from these tissues.

Arthroscopic evaluations during early stages of cartilage degeneration have additional limitations. They can be highly subjective as they rely on the perception of the surgeon performing the procedure. Several recent publications have expressed the feasibility of use of near infrared fiber optic probes during arthroscopy as a less subjective evaluation method^{1; 55; 57}. The use of near infrared probes has the potential to play an important role in monitoring early degeneration of cartilage for the high risk patients, such as those with anterior cruciate ligament or meniscus injury. Since the data obtained is less subjective than that from visual arthroscopy, more precise results on how to stage the cartilage may be obtained. In addition, the probability of success of novel therapies for OA likely depend on early diagnosis and thus earlier therapeutic intervention. Several disease modifying therapies are proposed in the literature to treat OA, such as non-drug therapies (exercise, weight loss), drug therapies (intra-articular corticosteroid injections, non-steroidal anti-inflammatory drugs (NSAIDs)⁵⁴, cell based therapies (stem cells injections)²⁰ and surgical procedures (debridement, microfracture^{25; 29}, autologous chondrocyte implantation (ACI)⁷. Near infrared fiber optic probe analysis could be a useful tool for assessment of therapeutic efficacy, as well as during debridement procedures to aid in determination of the margins of healthy versus degraded tissue areas.

Finally, non-destructive methods such as near infrared spectroscopy could prove to be an important tool not only in a clinical environment to detect early tissue degeneration, but also in a laboratory set up to understand disease progression. Many research groups are currently developing protocols for the growth of viable cartilage constructs for implantation, and these efforts would benefit greatly from non-destructive methods of analyses to assess the quality of cartilage constructs.

Conclusion

The results from this study confirm that the NIR absorbance band in cartilage at 5200 cm^{-1} arises from free and bound water, and the NIR absorbance band at 6890 cm^{-1} arises from bound water. The strong relation between either of the water bands with the absolute water content indicates that either of these can be used to assess water content in cartilage samples. These results lay the foundation for quantitative assessment of water changes in cartilage, which could be predictive of early tissue degeneration.

Acknowledgments

This study was supported by NIH AR056145 and EB00744 and the Intramural Research Program at NIA.

References

1. Afara I, Prasadam I, Crawford R, Xiao Y, Oloyede A. Non-destructive evaluation of articular cartilage defects using near-infrared (NIR) spectroscopy in osteoarthritic rat models and its direct relation to mankin score. *Osteoarthr Cartilage*. 2012
2. Afara I, Singh S, Oloyede A. Application of near infrared (NIR) spectroscopy for determining the thickness of articular cartilage. *Med Eng Phys*. 2012

3. Arimoto H, Egawa M. Non-contact skin moisture measurement based on near-infrared spectroscopy. *Appl Spectrosc.* 2004; 58:1439–1446. [PubMed: 15606957]
4. Arimoto H, Egawa M, Yamada Y. Depth profile of diffuse reflectance near-infrared spectroscopy for measurement of water content in skin. *Skin Res Technol.* 2005; 11:27–35. [PubMed: 15691256]
5. Armstrong CG V, Mow C. Variations in the intrinsic mechanical properties of human articular cartilage with age, degeneration, and water content. *J Bone Joint Surg Am.* 1982; 64:88–94. [PubMed: 7054208]
6. Bagratashvili VN, Sobol EN, Sviridov AP, Popov VK, Omel'chenko AI, Howdle SM. Thermal and diffusion processes in laser-induced stress relaxation and reshaping of cartilage. *J Biomech.* 1997; 30:813–817. [PubMed: 9239566]
7. Batty L, Dance S, Bajaj S, Cole BJ. Autologous chondrocyte implantation: An overview of technique and outcomes. *Anz Journal of Surgery.* 2011; 81:18–25. [PubMed: 21299794]
8. Baykal D, Irrechukwu O, Lin PC, Fritton K, Spencer RG, Pleshko N. Nondestructive assessment of engineered cartilage constructs using near-infrared spectroscopy. *Appl Spectrosc.* 2010; 64:1160–1166. [PubMed: 20925987]
9. Blanco M, Coello J, Iturriaga H, Maspoch S, de la Pezuela C. Near-infrared spectroscopy in the pharmaceutical industry. *Analyst.* 1998; 123:135R–150R.
10. Bock JE, Connelly RK. Innovative uses of near-infrared spectroscopy in food processing. *J Food Sci.* 2008; 73:R91–98. [PubMed: 18803725]
11. Brown CP, Bowden JC, Rintoul L, Meder R, Oloyede A, Crawford RW. Diffuse reflectance near infrared spectroscopy can distinguish normal from enzymatically digested cartilage. *Phys Med Biol.* 2009; 54:5579–5594. [PubMed: 19717892]
12. Brown CP, Jayadev C, Glyn-Jones S, Carr AJ, Murray DW, Price AJ, Gill HS. Characterization of early stage cartilage degradation using diffuse reflectance near infrared spectroscopy. *Phys Med Biol.* 2011; 56:2299–2307. [PubMed: 21411867]
13. Brown CP, Oloyede A, Crawford RW, Thomas GER, Price AJ, Gill HS. Acoustic, mechanical and near-infrared pro ling of osteoarthritic progression in bovine joints. *Phys Med Biol.* 2012; 57:14.
14. Büning-Pfaue H. Analysis of water in food by near infrared spectroscopy. *Food Chemistry.* 2003; 82:9.
15. Cachet T, Hoogmartens J. The determination of water in erythromycin by Karl Fischer titration. *J Pharm Biomed Anal.* 1988; 6:461–472. [PubMed: 16867392]
16. Canvin JM, Bernatsky S, Hitchon CA, Jackson M, Sowa MG, Mansfield JR, Eysel HH, Mantsch HH, El-Gabalawy HS. Infrared spectroscopy: Shedding light on synovitis in patients with rheumatoid arthritis. *Rheumatology (Oxford).* 2003; 42:76–82. [PubMed: 12509617]
17. Caplan AI, Elyaderani M, Mochizuki Y, Wakitani S, Goldberg VM. Principles of cartilage repair and regeneration. *Clin Orthop Relat Res.* 1997:254–269. [PubMed: 9308548]
18. Chan DD, Neu CP. Probing articular cartilage damage and disease by quantitative magnetic resonance imaging. *J R Soc Interface.* 2013; 10
19. Czarnik-Matusiewicz B, Pilorz S, Hawranek JP. Temperature-dependent water structural transitions examined by near-IR and mid-IR spectra analyzed by multivariate curve resolution and two-dimensional correlation spectroscopy. *Analytica Chimica Acta.* 2005; 544:15–25.
20. Diekman BO, Guilak F. Stem cell-based therapies for osteoarthritis: Challenges and opportunities. *Curr Opin Rheumatol.* 2013; 25:119–126. [PubMed: 23190869]
21. Dijkgraaf LC, de Bont LG, Boering G, Liem RS. Normal cartilage structure, biochemistry, and metabolism: A review of the literature. *J Oral Maxillofac Surg.* 1995; 53:924–929. [PubMed: 7629621]
22. Changhai, Ding; Cicuttini, F.; Jones, aG. How important is MRI for detecting early osteoarthritis? *Nat Clin Pract Rheumatol.* 2008; 4:4–5. [PubMed: 18030296]
23. Duda GN, Kleemann RU, Bluecher U, Weiler A. A new device to detect early cartilage degeneration. *Am J Sports Med.* 2004; 32:693–698. [PubMed: 15090387]
24. Esbensen, KH. Multivariate data analysis - in practice: An introduction to multivariate data analysis and experimental design. CAMO Software; Woodbridge: 2010.

25. Gill TJ. The treatment of articular cartilage defects using microfracture and debridement. *Am J Knee Surg.* 2000; 13:33. [PubMed: 11826923]
26. Hanifi A, Bi X, Yang X, Kavukcuoglu B, Lin PC, Dicarolo E, Spencer RG, Bostrom MP, Pleshko N. Infrared fiber optic probe evaluation of degenerative cartilage correlates to histological grading. *Am J Sports Med.* 2012
27. Hofmann GO, Marticke J, Grossstuck R, Hoffmann M, Lange M, Plettenberg HK, Braunschweig R, Schilling O, Kaden I, Spahn G. Detection and evaluation of initial cartilage pathology in man: A comparison between mrt, arthroscopy and near-infrared spectroscopy (NIR) in their relation to initial knee pain. *Pathophysiology.* 2010; 17:1–8. [PubMed: 19481428]
28. Howell, D. Etiopathogenesis of osteoarthritis. In: McCarty, DJ., editor. *Arthritis and allied conditions.* Lea and Febiger; Philadelphia: 1989.
29. Hunziker EB. Articular cartilage repair: Basic science and clinical progress. A review of the current status and prospects. *Osteoarthr Cartilage.* 2002; 10:432–463.
30. Jaffe FF, Mankin HJ, Weiss C, Zarins A. Water binding in the articular cartilage of rabbits. *J Bone Joint Surg Am.* 1974; 56:1031–1039. [PubMed: 4847225]
31. Koff MF, Amrami KK, Kaufman KR. Clinical evaluation of T2 values of patellar cartilage in patients with osteoarthritis. *Osteoarthr Cartilage.* 2007; 15:198–204.
32. Lawrence RC, Helmick CG, Arnett FC, Deyo RA, Felson DT, Giannini EH, Heyse SP, Hirsch R, Hochberg MC, Hunder GG, Liang MH, Pillemer SR, Steen VD, Wolfe F. Estimates of the prevalence of arthritis and selected musculoskeletal disorders in the united states. *Arthritis Rheum.* 1998; 41:778–799. [PubMed: 9588729]
33. Li G, Thomson M, Dicarolo E, Yang X, Nestor B, Bostrom MP, Camacho NP. A chemometric analysis for evaluation of early-stage cartilage degradation by infrared fiber-optic probe spectroscopy. *Appl Spectrosc.* 2005; 59:1527–1533. [PubMed: 16390593]
34. Fred, Libnau; Kvalheim, Olav M.; Christy, AA.; Toft, J. Spectra of water in the near- and mid-infrared region. *Vib Spectosc.* 1994; 7:243–254.
35. Lin PC, Reiter DA, Spencer RG. Classification of degraded cartilage through multiparametric MRI analysis. *J Magn Reson.* 2009; 201:61–71. [PubMed: 19762258]
36. Lin PC, Irrechukwu O, Roque R, Hancock B, Fishbein KW, Spencer RG. Multivariate analysis of cartilage degradation using the support vector machine algorithm. *Magn Reson Med.* 2011
37. Luck, WAP. In: Luck, WAP., editor. *Structure of water and aqueous solutions; Proceedings of the International Symposium; Marburg. July 1973; Marburg: 1974.*
38. Lusse S, Claassen H, Gehrke T, Hassenpflug J, Schunke M, Heller M, Gluer CC. Evaluation of water content by spatially resolved transverse relaxation times of human articular cartilage. *Magn Reson Imaging.* 2000; 18:423–430. [PubMed: 10788720]
39. Mankin HJ, Thrasher AZ. Water content and binding in normal and osteoarthritic human cartilage. *J Bone Joint Surg Am.* 1975; 57:76–80. [PubMed: 1123375]
40. Marik W, Apprich S, Welsch G, Mamisch T, Trattng S. Biochemical evaluation of articular cartilage in patients with osteochondrosis dissecans by means of quantitative T2- and T2*-mapping at 3t MRI: A feasibility study. *European Journal of Radiology.* 2012; 81:923–927. [PubMed: 21392912]
41. Maroudas A. Distribution and diffusion of solutes in articular cartilage. *Biophys J.* 1970; 10:365–379. [PubMed: 4245322]
42. Maroudas A, Bayliss MT, Uchitel-Kaushansky NaSR. Aggrecan turnover in human articular cartilage: Use of aspartic acid racemization as a marker of molecular age. *Arch Biochem Biophys.* 1998; 350:61–71. [PubMed: 9466821]
43. Marticke JK, Hosselbarth A, Hoffmeier KL, Marintschev I, Otto S, Lange M, Plettenberg HK, Spahn G, Hofmann GO. How do visual, spectroscopic and biomechanical changes of cartilage correlate in osteoarthritic knee joints? *Clin Biomech (Bristol, Avon).* 2010; 25:332–340.
44. Martin K. In vivo measurements of water in skin by near-infrared reflectance. *Appl Spectrosc.* 1998; 52:1001–1007.
45. Nicolai BM, Beullens K, Bobelyn E, Peirs A, Saeys W, Theron KI, Lammertyn J. Nondestructive measurement of fruit and vegetable quality by means of NIR spectroscopy: A review. *Postharvest Biol Tec.* 2007; 46:99–118.

46. O'Malley MJ, Chu CR. Arthroscopic optical coherence tomography in diagnosis of early arthritis. *Minim Invasive Surg.* 2011; 2011
47. Peterfy CG. Scratching the surface: Articular cartilage disorders in the knee. *Magn Reson Imaging Clin N Am.* 2000; 8:409–430. [PubMed: 10819921]
48. Platt D, Bird JL, Bayliss MT. Ageing of equine articular cartilage: Structure and composition of aggrecan and decorin. *Equine Vet J.* 1998; 30:43–52. [PubMed: 9458398]
49. Poole AR, Kojima T, Yasuda T, Mwale F, Kobayashi M, Laverty S. Composition and structure of articular cartilage: A template for tissue repair. *Clin Orthop Relat Res.* 2001:S26–33. [PubMed: 11603710]
50. Recht MP, Goodwin DW, Winalski CS, White LM. MRI of articular cartilage: Revisiting current status and future directions. *AJR Am J Roentgenol.* 2005; 185:899–914. [PubMed: 16177408]
51. Reiter DA, Lin PC, Fishbein KW, Spencer RG. Multicomponent T2 relaxation analysis in cartilage. *Magn Reson Med.* 2009; 61:803–809. [PubMed: 19189393]
52. Ressler N, Ziauddin, Vygantas C, Janzen W, Karachorlu K. Improved techniques for near-infrared study of water binding by globular proteins and intact tissues. *Appl Spectrosc.* 1976; 30:295–302.
53. Shiomi T, Nishii T, Nakata K, Tamura S, Tanaka H, Yamazaki Y, Murase K, Yoshikawa H, Sugano N. Three-dimensional topographical variation of femoral cartilage T2 in healthy volunteer knees. *Skeletal Radiol.* 2012:1–8. [PubMed: 22072236]
54. Sovani S, Grogan SP. Osteoarthritis: Detection, pathophysiology, and current/future treatment strategies. *Orthop Nurs.* 2013; 32:25–36. [PubMed: 23344487]
55. Spahn G, Plettenberg H, Kahl E, Klinger HM, Muckley T, Hofmann GO. Near-infrared (NIR) spectroscopy. A new method for arthroscopic evaluation of low grade degenerated cartilage lesions. Results of a pilot study. *BMC Musculoskelet Disord.* 2007; 8:47. [PubMed: 17535439]
56. Spahn G, Plettenberg H, Nagel H, Kahl E, Klinger HM, Gunther M, Muckley T, Hofmann GO. Karl Fischer titration and coulometry for measurement of water content in small cartilage specimens. *Biomed Tech (Berl).* 2006; 51:355–359. [PubMed: 17155872]
57. Spahn G, Plettenberg H, Nagel H, Kahl E, Klinger HM, Muckley T, Gunther M, Hofmann GO, Mollenhauer JA. Evaluation of cartilage defects with near-infrared spectroscopy (NIR): An ex vivo study. *Med Eng Phys.* 2008; 30:285–292. [PubMed: 17553725]
58. Torzilli, PA. Water content and solute diffusion properties in articular cartilage. Springer-Verlag; New York: 1990.
59. Torzilli PA, Adams TC, Mis RJ. Transient solute diffusion in articular cartilage. *J Biomech.* 1987; 20:203–214. [PubMed: 2437125]
60. Vandermeulen DL, Ressler N. A near-infrared analysis of water-macromolecule interactions: Hydration and the spectra of aqueous solutions of intact proteins. *Arch Biochem Biophys.* 1980; 199:197–205. [PubMed: 6766705]
61. Walling PL, Dabney JM. Moisture in skin by near-infrared reflectance spectroscopy. *J Soc Cosmet Chem.* 1989; 40:151–171.
62. Wei L, Svensson O, Hjerpe A. Correlation of morphologic and biochemical changes in the natural history of spontaneous osteoarthrosis in guinea pigs. *Arthritis Rheum.* 1997; 40:2075–2083. [PubMed: 9365098]
63. West PA, Bostrom MP, Torzilli PA, Camacho NP. Fourier transform infrared spectral analysis of degenerative cartilage: An infrared fiber optic probe and imaging study. *Appl Spectrosc.* 2004; 58:376–381. [PubMed: 15104805]
64. Xia Y. MRI of articular cartilage at microscopic resolution. *BJR.* 2013; 2:9–17. [PubMed: 23610697]
65. Yin J, Xia Y. Macromolecular concentrations in bovine nasal cartilage by fourier transform infrared imaging and principal component regression. *Appl Spectrosc.* 2010; 64:1199. [PubMed: 21073787]
66. Zhou GX, Ge Z, Dorwart J, Izzo B, Kukura J, Bicker G, Wyrvatt J. Determination and differentiation of surface and bound water in drug substances by near infrared spectroscopy. *J Pharm Sci.* 2003; 92:1058–1065. [PubMed: 12712426]

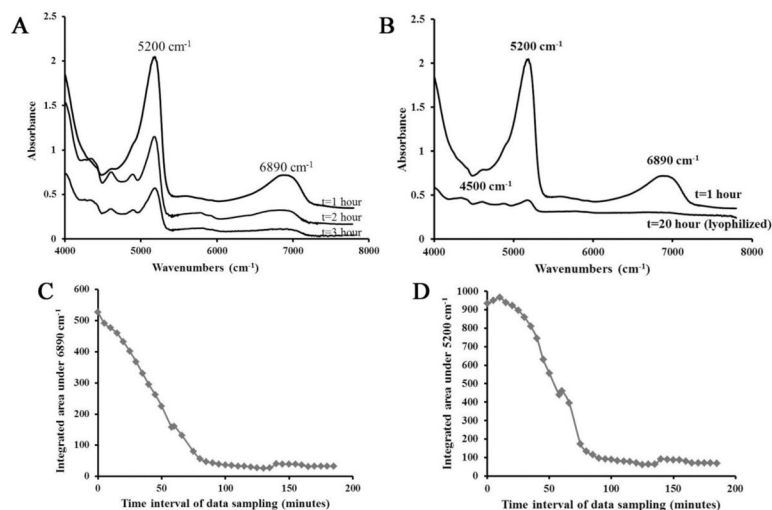


Figure 1.

Absorbance spectra obtained from BNC. A) A decrease in the 5200 cm^{-1} and 6890 cm^{-1} absorbances is observed in spectra acquired at 5 minute intervals over 3 hours, reflecting evaporation of water. The spectra are offset to illustrate the differences, with earlier time point spectra above and later time point spectra below. B) NIR spectra from a BNC sample after one hour of drying and from a lyophilized sample. The NIR absorbance at 5200 cm^{-1} arises from “free and bound” water and the NIR absorbance at 6890 cm^{-1} arises from “free” water. Decrease in integrated area under NIR absorbance at C) 5200 cm^{-1} and D) 6890 cm^{-1} obtained from BNC samples imaged at 5 minutes intervals.

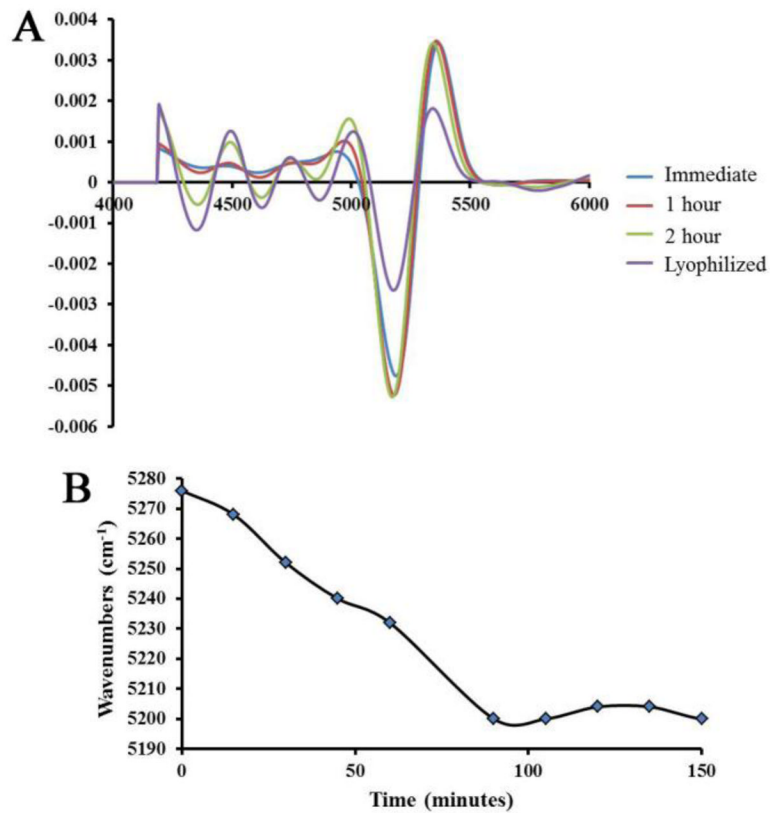


Figure 2.

A) Second derivative spectra obtained from 1 mm thick BNC sections as water evaporates over time (spectra acquired immediately, after 1 hour, 2 hours, and after lyophilization). More features are observed in the lower frequency regions (attributed to matrix absorbances) as water evaporates. B) A shift to a lower frequency is observed in the NIR absorbance band centered at $\sim 5200 \text{ cm}^{-1}$ as water evaporates over time.

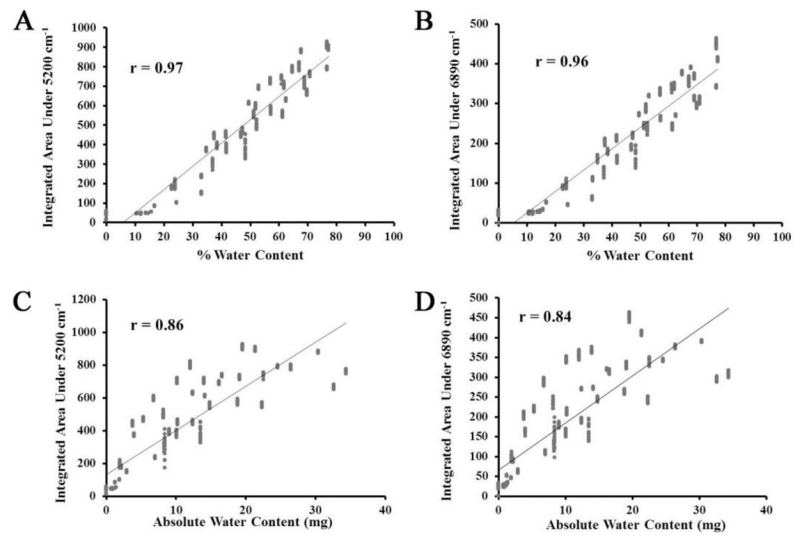


Figure 3.

Correlation between gravimetrically determined percent water content of 0.5 mm thick BNC samples and integrated area under the A) 5200 cm⁻¹ and B) 6890 cm⁻¹ absorbances.

Correlation between absolute water content of 0.5 mm thick BNC samples and integrated area under the C) 5200 cm⁻¹ and D) 6890 cm⁻¹ absorbances.

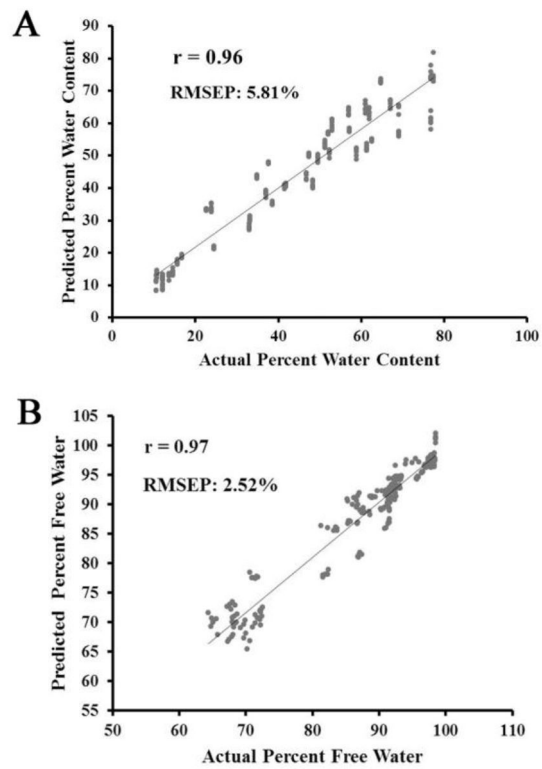


Figure 4.

A) Predicted vs. actual percent water content obtained from a partial least squares regression model using BNC tissues dried over a three hour period. B) Predicted vs. actual percent free water content obtained from a partial least squares regression model using BNC tissues dried over a three hour period.

Table 1

Averaged parameters of PLS models* of NIR spectra for prediction of absolute, percent and free water content in hyaline cartilage.

PLS Parameter	Absolute water (mg)	Percent water	Percent water (Physiological region)	Percent free water
A R ² of test model (calibration)	0.86±0.008	0.92	0.89±0.009	0.93±0.004
B RMSE	2.8±0.094	5.80±0.012	2.6±0.130	2.45±0.0326
C R ² of validation	0.84±0.012	0.92±0.0003	0.88±0.0007	0.94±0.002
D Correlation Coefficient	0.92±0.004	0.96±0.0002	0.94±0.003	0.97±0.001
E Factors	7	1	7	4
F RMSEP	3.05 ±0.113mg	5.81±0.012%	2.68±0.125	2.51±0.023%

* MSC-corrected second derivative spectra (420) were used in each model, and data is presented for n = 3 models, ± standard deviation. Parameters A to E, were calculated from the cross-validation models. Root mean square (RMSE) of validation was measured to determine the overall error of the model. Parameter F, the root mean square error of prediction (RMSEP), was calculated from the independent prediction of the remaining 252 spectra.